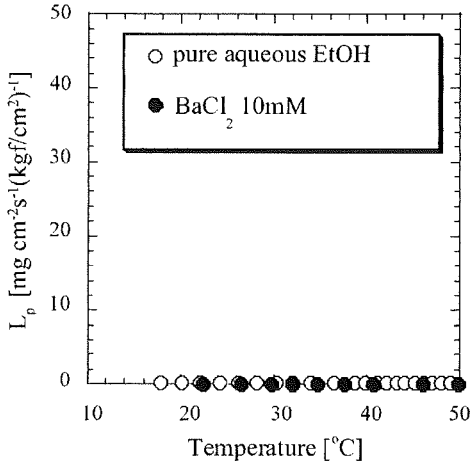

Fig. 9. Temperature dependence of the permeability coefficient of aqueous ethanol solutions containing 10 mM $BaCl_2$ or no ion. Concentration of ethanol was 26.1 mol% in both cases.

To compare the sensitivity of the membrane to $BaCl_2$ in a more direct way, the dependence of the permeation flux on $BaCl_2$ concentration was investigated in aqueous 19.6 mol% ethanol solution and pure water, together with that on $CaCl_2$ concentration at a temperature that was 10 °C higher than each LCST (Fig. 11). In the case of the ethanol solution, the permeation flux decreased from 1 mM $BaCl_2$ to 10 mM $BaCl_2$, while it decreased from 10 mM $BaCl_2$ to 100 mM $BaCl_2$. Thus, the sensitivity of the membrane to $BaCl_2$ in the aqueous ethanol solution is roughly 10 times higher than that in the aqueous solution. The concentration of $CaCl_2$ did not change the permeation flux, which shows that this phenomenon occurred as a result of molecular recognition by the crown ether receptors. This high sensitivity and stability of the membrane and its response in solutions containing organic solvents are unique and expected to

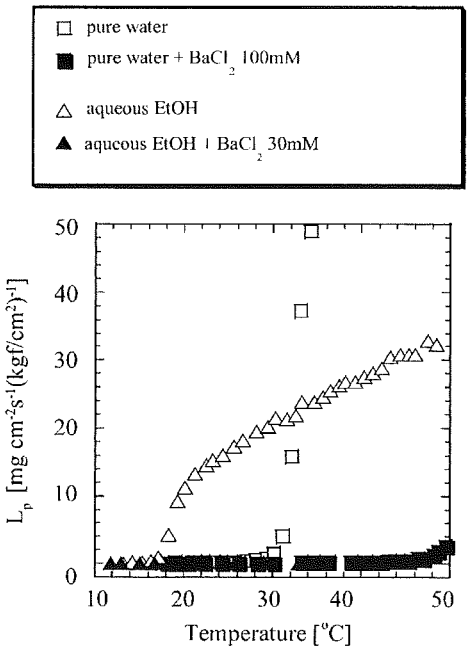

Fig. 10. Temperature dependence of the permeability coefficient of water (0 mol%) or aqueous ethanol solution (19.6 mol%) containing $BaCl_2$ through a molecular recognition ion gating membrane. Except for the plots of aqueous 100 mM $BaCl_2$, all of the data have already been shown in Figs. 4 and 6.

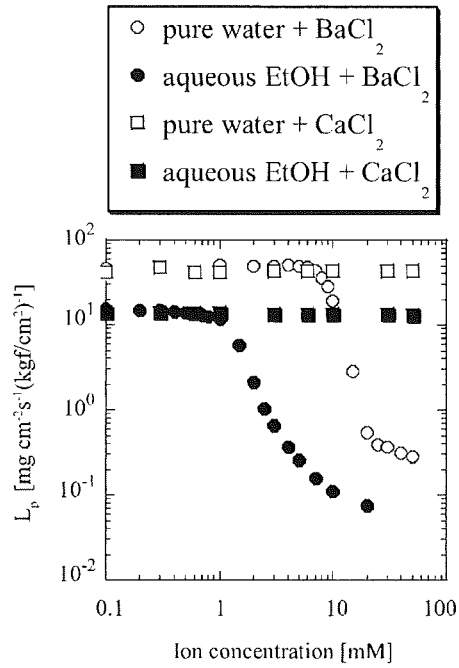

Fig. 11. Ion concentration dependence of the permeability coefficient of aqueous ethanol solutions (19.6 mol%) or water (0 mol%) containing $BaCl_2$ or $CaCl_2$ through a molecular recognition ion gating membrane. Temperature was 39.5 °C for the 19.6 mol% aqueous solution and 27.3 °C for pure water.

be applied to the gating membrane for sensing materials in the engineering field in future.

In terms of the phase diagram of Fig. 4, the globule-state region at around 15 mol% of ethanol is a quite sensitive region to respond to ion signals. These phenomena can probably be explained in terms of the complex formation constant of the crown ether moiety of BCAm in the grafted copolymer. Complex formation constants of benzo[18]crown-6 with inorganic ions have been previously reported to increase with increasing methanol mole ratio in aqueous methanol solution (Log K between benzo[18]crown-6 and K^+: 1.84, 3.82, 4.75 and 5.29 at 0, 70, 80, 90 and 100 wt% of methanol [30]). We also reported that the complex formation constant of the crown ether moiety of BCAm increased with increasing methanol mole ratio in aqueous methanol solution (Log K between BCAm and K^+: 1.0, 2.2, 2.9 and 3.5 at 0, 70, 80, 90 and 100 wt% of methanol [29]). Although detailed data on the complex formation constants of benzo[18]crown-6 in aqueous ethanol solution have not been reported to our knowledge, the tendency in the case of ethanol can reasonably be assumed to be similar to that in the case of methanol. In addition, the sensitivity enhancement of the crown ether receptors occurred by the increase in complex formation constant with increasing ethanol ratio.

We can understand the sensitivity enhancement roughly as described above, but the detailed mechanism needs to be investigated more deeply. The mechanism for the reentrant phase transition of poly-NIPAM is not yet clear, because water, ethanol and poly-NIPAM interact with each other in a complicated manner; thus, the effect of complexation between BCAm and a signal ion on the reentrant phase transition at the LCSTs is complicated, and further research is required.

4. Conclusions

We investigated both the reentrant phase transition of linear poly-NIPAM-co-BCAm and the response of a molecular recognition

ion gating membrane to signal ions in aqueous ethanol solutions. The reentrant phase transition of poly-NIPAM-co-BCAm showed LCST/LCST-type behavior in ethanol, which is different from the previous report of poly-NIPAM. In addition, the phase diagram of poly-NIPAM-co-BCAm changed because of the stimuli of the ion signal. According to this unique reentrant phase transition behavior of poly-NIPAM-co-BCAm, the gating membrane repeatedly and stably responded to ion signals in the mixed solvent of ethanol and water, because the gating membrane was prepared using synthetic polymers only. We also found that sensitivity and selectivity of the gating membrane to ion species changed in aqueous ethanol solution and, in particular, the sensitivity was enhanced by the addition of ethanol, which can be triggered by the increase of complex formation constant with increasing ethanol mole ratio in the solution.

References

[1] T. Ito, T. Hioki, T. Yamaguchi, T. Shinbo, S. Nakao, S. Kimura, Development of a molecular recognition ion gating membrane and estimation of its pore size control, J. Am. Chem. Soc. 124 (2002) 7840.

[2] T. Ito, T. Yamaguchi, Osmotic pressure control in response to a specific ion signal at physiological temperature using a molecular recognition ion gating membrane, J. Am. Chem. Soc. 126 (2004) 6202.

[3] T. Ito, T. Yamaguchi, Nonlinear self-excited oscillation of a synthetic ion-channel-inspired membrane, Angew. Chem., Int. Ed. 45 (2006) 5630.

[4] O. Schepelina, I. Zharov, PNIPAAM-modified nanoporous colloidal films with positive and negative temperature gating, Langmuir 23 (2007) 12704.

[5] D. Lee, A.J. Nolte, A.L. Kunz, M.F. Rubner, R.E. Cohen, pH-induced hysteretic gating of track-etched polycarbonate membranes: swelling/deswelling behavior of polyelectrolyte multilayers in confined geometry, J. Am. Chem. Soc. 128 (2006) 8521.

[6] L.Y. Chu, Y. Li, J.H. Zhu, W.M. Chen, Negatively thermoresponsive membranes with functional gates driven by zipper-type hydrogen-bonding interactions, Angew. Chem., Int. Ed. 44 (2005) 2124.

[7] M. Asano, F.M. Winnik, T. Yamashita, K. Horie, Fluorescence studies of dansyl-labeled poly(*N*-isopropylacrylamide) gels and polymers in mixed water/methanol solutions, Macromolecules 28 (1995) 5861.

[8] Y. Osada, Y. Takeuchi, Protein and sugar separation by mechanochemical membrane having chemical valve function, Polym. J. 15 (1983) 279.

[9] K. Ishihara, M. Kobayashi, I. Shionohara, Control of insulin permeation through a polymer membrane with responsive function for glucose, Makromol. Chem. Rapid Commun. 4 (1983) 327.

[10] Y. Osada, Y. Takeuchi, Water and protein permeation through polymeric membrane having mechanochemically expanding and contracting pores—function of chemical valve 1, J. Polym. Sci., Part C: Polym. Lett. 19 (1981) 303.

[11] T. Miyata, N. Asami, T. Uragami, A reversibly antigen-responsive hydrogel, Nature 399 (1999) 766.

[12] Y.S. Park, Y. Ito, Y. Imanishi, Permeation control through porous membranes immobilized with thermosensitive polymer, Langmuir 14 (1998) 910.

[13] Y. Ito, Y.S. Park, Y. Imanishi, Nanometer-sized channel gating by a self-assembled polypeptide brush, Langmuir 16 (2000) 5376.

[14] K. Ishihara, M. Kobayashi, N. Ishimaru, I. Shinohara, Glucose-induced permeation control of insulin through a complex membrane consisting of immobilized glucose-oxidase and a poly(amine), Polym. J. 16 (1984) 625.

[15] H.G. Schild, M. Muthukumar, D.A. Tirrell, Cononsolvency in mixed aqueous solutions of poly(*N*-isopropylacrylamide), Macromolecules 24 (1991) 948.

[16] F.M. Winnik, M.F. Ottaviani, S.H. Bossmann, M. Garciagaribay, N.J. Turro, Cononsolvency of poly(*N*-isopropylacrylamide) in mixed water–methanol solutions—a look at spin-labeled polymers, Macromolecules 25 (1992) 6007.

[17] K. Mukae, M. Sakurai, S. Sawamura, K. Makino, S.W. Kim, I. Ueda, K. Shirahama, Swelling of poly(*N*-isopropylacrylamide) gels in water–alcohol (C1–C4) mixed solvents, J. Phys. Chem. 97 (1993) 737.

[18] P.W. Zhu, D.H. Napper, Coil-to-globule type transitions and swelling of poly(*N*-isopropylacrylamide) and poly(acrylamide) at latex interfaces in alcohol–water mixtures, J. Colloid Interf. Sci. 177 (1996) 343.

[19] A. Acharya, A. Goswami, P.K. Pujari, S. Sabharwal, S.B. Manohar, Positron annihilation studies of poly(*N*-isopropyl acrylamide) gel in mixed solvents, J. Polym. Sci., Part A: Polym. Chem. 40 (2002) 1028.

[20] R.O.R. Costa, R.F.S. Freitas, Phase behavior of poly(*N*-isopropylacrylamide) in binary aqueous solutions, Polymer 43 (2002) 5879.

[21] W. Hyk, M. Ciszkowska, Preparation and electrochemical characterization of poly(*N*-isopropylacrylamide-co-acrylic acid) gels swollen by nonaqueous solvents: alcohols, J. Phys. Chem. B 106 (2002) 11469.

[22] G.M. Liu, G.Z. Zhang, Reentrant behavior of poly(*N*-isopropylacrylamide) brushes in water–methanol mixtures investigated with a quartz crystal microbalance, Langmuir 21 (2005) 2086.

[23] I. Alenichev, Z. Sedlakova, M. Ilavsky, Swelling and mechanical behavior of charged poly(*N*-isopropylmethacrylamide) and poly(*N*-isopropylacrylamide) networks in water/ethanol mixtures. Cononsolvency effect, Polym. Bull. 58 (2007) 191.

[24] R. Kita, P. Polyakov, S. Wiegand, Ludwig–Soret effect of poly(*N*-isopropylacrylamide): temperature dependence study in monohydric alcohols, Macromolecules 40 (2007) 1638.

[25] H. Yamauchi, Y. Maeda, LCST and UCST behavior of poly(*N*-isopropylacrylamide) in DMSO/water mixed solvents studied by IR and micro-Raman spectroscopy, J. Phys. Chem. B 111 (2007) 12964.

[26] M. Irie, Y. Misumi, T. Tanaka, Stimuli-responsive polymers—chemical induced reversible phase separation of an aqueous solution of poly(*N*-isopropylacrylamide) with pendant crown ether groups, Polymer 34 (1993) 4531.

[27] R. Ungaro, B.E. Haj, J. Smid, Substituent effects on stability of cation complexes of 4′-substituted monobenzo crown ethers, J. Am. Chem. Soc. 98 (1976) 5198.

[28] K. Yagi, J.A. Ruiz, M.C. Sanchez, Cation binding properties of polymethacrylamide derivatives of crown ethers, Makromol. Chem. Rapid Commun. 1 (1980) 263.

[29] T. Ito, Y. Sato, T. Yamaguchi, S. Nakao, Response mechanism of a molecular recognition ion gating membrane, Macromolecules 37 (2004) 3407.

[30] R.M. Izatt, K. Pawlak, J.S. Bradshaw, R.L. Bruening, Thermodynamic and kinetic data for macrocycle interaction with cations and anions, Chem. Rev. 91 (1991) 1721.

[31] G. Zhang, C. Wu, Reentrant coil-to-globule-to-coil transition of a single linear homopolymer chain in a water/methanol mixture, Phys. Rev. Lett. 86 (2001) 822.

[32] G. Zhang, C. Wu, The water/methanol complexation induced reentrant coil-to-globule-to-coil transition of individual homopolymer chains in extremely dilute solution, J. Am. Chem. Soc. 123 (2001) 1376.

[33] Y. Okada, F. Tanaka, Cooperative hydration, chain collapse, and flat LCST behavior in aqueous poly(*N*-isopropylacrylamide) solutions, Macromolecules 38 (2005) 4465.

[34] F. Tanaka, T. Koga, Temperature-responsive polymers in mixed solvent: competitive hydrogen bonds cause cononsolvency, Phys. Rev. Lett. 101 (2008) 028302.

[35] F. Tanaka, T. Koga, H. Kojima, F.M. Winnik, Temperature- and tension-induced coil–globule transition of poly(*N*-isopropylacrylamide) chains in water and mixed solvent of water/methanol, Macromolecules 42 (2009) 1321.

[36] Y. Ito, T. Ito, H. Takaba, S. Nakao, Development of gating membranes that are sensitive to the concentration of ethanol, J. Membr. Sci. 261 (2005) 145.

Analysis of Pore Size Using a Straight-Pore Molecular Recognition Ion Gating Membrane

Naoko MIYAOI[1], Hidenori OHASHI[1],
Taichi ITO[2] and Takeo YAMAGUCHI[1,2]
[1]*Department of Chemical System Engineering, The University of Tokyo, 7-3-1, Hongo, Bunkyo-ku, Tokyo 113-8656, Japan*
[2]*Chemical Resources Laboratory, Tokyo Institute of Technology, R1-17, 4259, Nagatsuta-cho, Midori-ku, Yokohama-shi, Kanagawa 226-8503, Japan*

Keywords: Molecular Recognition, Ion Gating Membrane, Cylindrical Pore, Water Permeability, Hagen–Poiseuille Equation

An analysis of the water permeability of a molecular recognition ion gating membrane was performed. The ion gating membrane shows outstanding water permeability switching properties in response to specific ion concentrations, using an ion-responsive polymer consisting of thermosensitive poly(*N*-isopropylacrylamide) and crown ether moieties, grafted onto a porous substrate pore surface. To investigate the precise properties of the membrane, a polycarbonate track-etched membrane having straight pores with a narrow pore size distribution was used as the substrate, and the ion responsive polymer was grafted onto its pore surfaces. The gating property of the prepared membrane was examined as a function of temperature, specific ion concentration, and filling ratio. Estimates of pore size and dimension of the grafted polymer were obtained using the Hagen–Poiseuille equation. We found that the grafted ion-responsive polymer shows drastic dimensional changes in response to temperature and specific ion concentrations.

Introduction

The living body is a sophisticated system that expresses a range of diverse and outstanding functions. Methodologies to develop analogous functional systems using pure artificial materials are inspired by this biosystem, and this strategy is promising. Molecular recognition functionality is one of the key elements required to design distinct systems in living bodies and also in artificial devices.

Following this strategy, we have proposed a molecular recognition ion gating membrane (Yamaguchi *et al.*, 1999; Ito *et al.*, 2002). This sophisticated membrane consists of a porous membrane as a stable substrate and a grafted polymer as the ion-responsive moiety (**Figure 1**). The grafted polymer is a copolymer of *N*-isopropylacrylamide (NIPAM), which has thermoresponsive properties, and benzo-18-crown-6 acrylamide (BCAm), which recognizes specific ions (such as K^+ and Ba^{2+}) (Irie *et al.*, 1993). The ion gating membrane can close its pores in the presence of the specific ion, and can open them in the absence of that ion. The membrane shows marked ability to control water permeability in response to specific ion concentrations. However, the substrate used in the previous investigations was porous polyethylene (PE), which has complex pores and a wide pore size distribution (Yamaguchi *et al.*, 1999; Ito *et al.*, 2002), and precise information is required for analysis and application of the ion gating membrane.

Therefore, we prepared an ion gating membrane for this study using a polycarbonate track-etched membrane with straight pores and a narrow pore size distribution (Rui *et al.*, 2005; Friebe and Ulbricht, 2007) as the porous substrate, and performed an analysis of the membrane's water permeability and pore size as a function of temperature, ionic concentration, and filling ratio.

1. Experimental

1.1 Materials

Cyclopore® polycarbonate, track-etched with a porosity of 17% was used as the porous substrate, and purchased from SPI Supplies Division of Structure Probe, Inc. BCAm was synthesized from benzo-18-crown-6 using published techniques (Ungaro *et al.*, 1976; Yagi *et al.*, 1980). Benzo-18-crown-6 was purchased from Sigma-Aldrich Japan K.K., and barium chloride ($BaCl_2$) and *N*-dodecylbenzenesulfonic acid

Received on January 15, 2008; accepted on February 25, 2008.
Correspondence concerning this article should be addressed to H. Ohashi (E-mail address: hidenori@chemsys.t.u-tokyo.ac.jp).

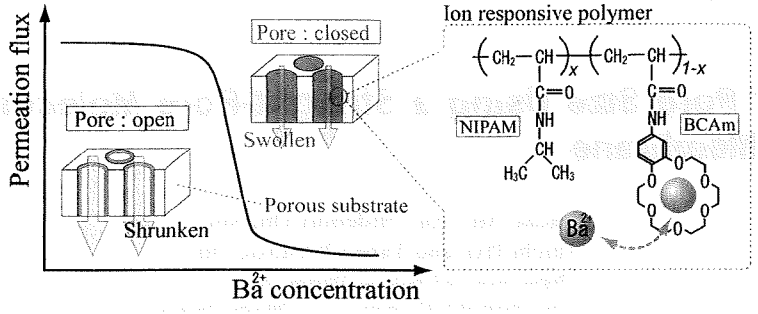

Fig. 1 Schematic representation of a molecular recognition ion gating membrane

sodium salt (SDBS) were purchased from Wako Pure Chemical Industries, Ltd. NIPAM was supplied by Kohjin Co., Ltd.

1.2 Preparation of an ion gating membrane having cylindrical pores and uniform pore size distribution

An ion gating membrane having cylindrical straight pores and uniform pore size distribution was prepared using the track-etched membrane and the plasma graft polymerization technique developed in our previous work (Yamaguchi *et al.*, 1991, 1996). The Cyclopore® was treated with argon plasma at a pressure of 10 Pa, and was then exposed to air for 60 s to generate peroxide groups on its pore surface. The substrate containing peroxide groups was immersed in an extensively degassed (frozen and thawed) aqueous solution of 5 wt% monomers of NIPAM and BCAm (the molar ratio of NIPAM to BCAm was fixed at 95:5), and 4 wt% SDBS as a surfactant. By holding the solution at 80°C, the peroxide groups were broken to form active radical sites, and a graft polymerization reaction started from the initiator radicals. The reaction time was varied from 10 to 60 min to control the filling ratio. After the grafting, any remaining monomers and surfactant were removed by rinsing the membrane with water, a 50% aqueous ethanol solution, and hexane for 1 h, respectively. Graft polymerization was evaluated by weight change, FT–IR spectra, and scanning electron microscopy (SEM). The filling ratio ϕ of the grafted membrane is defined by Eq. (1).

$$\phi\,[\%] = \frac{W_{dry} - W_{sub}}{\rho_{polym} \cdot V_{pore}} \times 100 \qquad (1)$$

where, W_{dry} [g] and W_{sub} [g] represent the weight of the grafted membrane and the nongrafted membrane substrate, respectively. ρ_{polym} [g/cm^3] is the density of the ion-responsive polymer, and is assumed to be 1.0 g/cm^3 for a copolymer of NIPAM and BCAm. V_{pore} [cm^3] is the pore volume of the substrate.

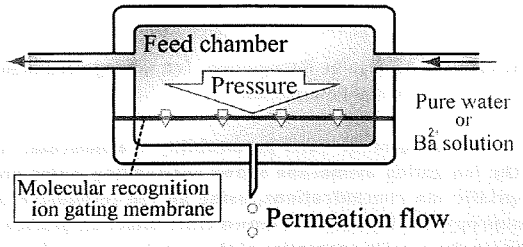

Fig. 2 Filtration apparatus to measure the permeation flux through a molecular recognition ion gating membrane

1.3 Measurement of permeation flux through the prepared molecular recognition ion gating membrane

The water permeation flux through the prepared ion gating membrane was measured. A schematic diagram of the filtration apparatus to measure the permeation flow is shown in **Figure 2**. Pure water or an aqueous $BaCl_2$ solution was passed through a feed chamber and an appropriate pressure (0.18–0.22 kg f/cm^2) was applied across the membrane. The permeation flux was calculated from the amount of permeated solution. Here, to eliminate the effect of the applied pressure and media viscosity on permeation flux J [m^3/(s cm^{-2})], the permeability coefficient L_p [m/(kg f s cm^{-2})] was used to evaluate membrane permeability. L_p is defined in Eq. (2).

$$L_p = \frac{J}{\Delta P \cdot \left(\mu_{25^\circ C}/\mu_T\right)} \qquad (2)$$

where, ΔP [kg f/m^2] is the pressure applied across the membrane, and $\mu_{25^\circ C}$ [Pa s] and μ_T [Pa s] represent media viscosity at 25°C and the measurement temperature, respectively. In this series of measurements, the $BaCl_2$ concentration was varied from 1 to 100 mM, the measurement temperature was varied from 20 to 50°C, and the filling ratio was varied from 0 to 37%.

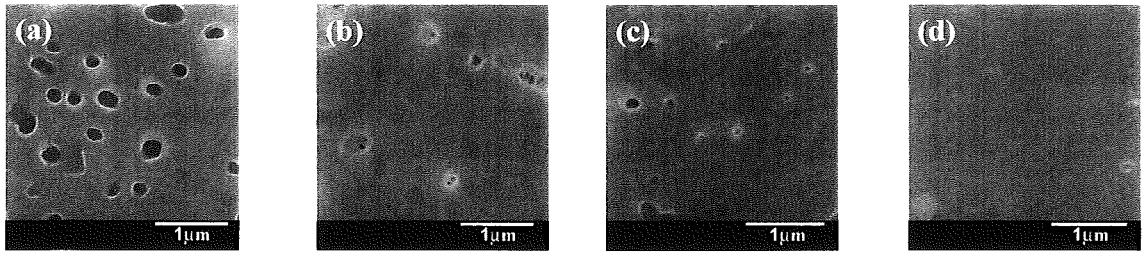

Fig. 3 Scanning electron microscopy images of poly (NIPAM-co-BCAm) grafted polycarbonate track-etched membrane; filling ratio (a) 0% (nongrafted), (b) 13.9%, (c) 31.0%, and (d) 73.4%

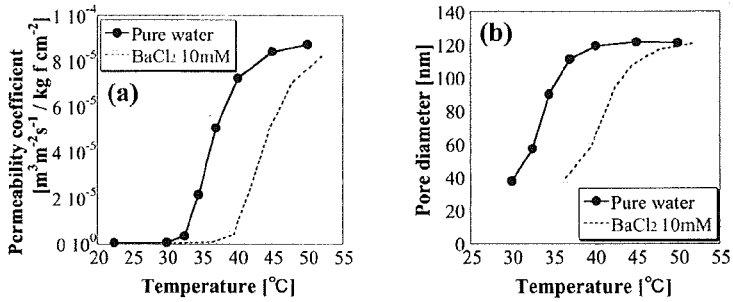

Fig. 4 Temperature dependence of permeation properties on an ion gating membrane having cylindrical straight pores (filling ratio 15.3%) for pure water and 10 mM aqueous $BaCl_2$ solution: (a) permeability coefficient; (b) pore diameter

2. Results and Discussion

2.1 Preparation of an ion gating membrane having cylindrical pores and uniform pore size distribution

From the weight difference measured before and after the graft polymerization, FT–IR spectra, and SEM images, successful polymer grafting on the PCTE substrate was confirmed. SEM images of the grafted membranes with several filling ratios are shown in the dry state in **Figure 3**. It can be seen that the pore size of the membrane becomes smaller as the filling ratio increases. With a filling ratio of 73%, the pores were almost completely filled with grafting polymer, even in their dry state. The figure also shows successful grafting on the membrane pore surface.

2.2 Measurement of permeation flux through the prepared molecular recognition ion gating membrane

The temperature dependence of the permeability coefficient for pure water and a 10 mM aqueous $BaCl_2$ solution is shown in **Figure 4(a)**. A membrane with a 15.3% filling ratio was used. Both lines show clear lower critical solution temperature (LCSTs), where the permeability drastically changes. In the presence of Ba^{2+} ions, the LCST shifts to a higher temperature. The observed LCSTs are almost the same as the LCSTs of the membrane prepared using a PE substrate (Ito *et al.*, 2002). To examine the effect of Ba^{2+} ions on the gating property of the membrane, the $BaCl_2$ concentration dependence of the permeability at 37°C was also investigated. As shown in **Figure 5(a)**, as the $BaCl_2$ concentration increases, the permeation flux decreases. Above 10 mM $BaCl_2$, the permeability decreases greatly. The tendency is again similar to that of the membrane prepared using the PE substrate. Furthermore, the filling ratio dependence of the permeability at the presence and absence of $BaCl_2$ at 37°C is shown in **Figure 6(a)**. The permeation flux decreases as the filling ratio increases, in both pure water and the 10 mM aqueous $BaCl_2$ solution. This indicates that pore size is reduced by increases in the amount of graft polymer, and coincides with the trend seen in the SEM image shown in Figure 3.

2.3 Analysis of pore size of the ion gating membrane with cylindrical straight pores

The ion gating membrane prepared with Cyclopore® should have straight pores with a narrow pore size distribution. Therefore, the pore diameter can be calculated from the permeation flux shown in Figures 4(a) to 6(a), using the Hagen–Poiseuille equation, which is valid for cylindrical straight pores. The permeation flux J in the Hagen–Poiseuille equation can be represented by Eq. (3).

$$J = \frac{\varepsilon \cdot \Delta P \cdot d^4}{32\mu \cdot L \cdot d_0^2} \tag{3}$$

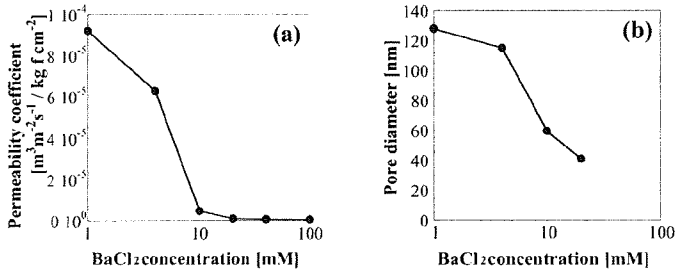

Fig. 5 $BaCl_2$ concentration dependence of membrane permeation properties (filling ratio 15.3%) at 37°C: (a) permeability coefficient; (b) pore diameter

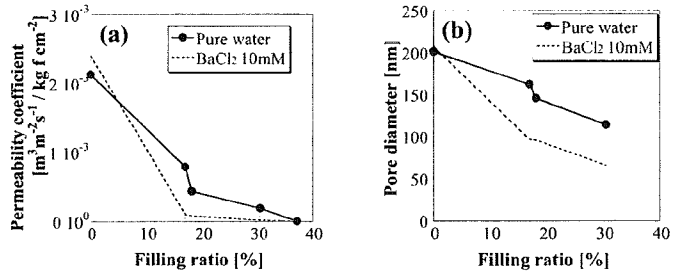

Fig. 6 Filling ratio dependence of membrane permeation properties for pure water and 10 mM aqueous $BaCl_2$ solution at 37°C: (a) permeability coefficient; (b) pore diameter

where, d [m] and d_0 [m] represent the pore diameter of the grafted and nongrafted membranes, respectively. L [m] and ε [—] are the thickness and porosity of the substrate. The permeation flux has a fourth power dependency on pore diameter, because the pore number density is always constant. We note that at low permeabilities, the relationship between permeability and pore size is more complex, given that the pore sizes will be less uniform because the distribution of the degree of polymerization and the fluctuation of polymer dimension may not satisfy the conditions of Eq. (3). Thus, we avoided the application of the equation at low permeabilities. The pore diameters derived from the permeation fluxes using the Hagen–Poiseuille equation are shown in **Figures 4(b)** to **6(b)**.

The validity of the evaluation is confirmed since the pore diameter calculated for the nongrafted membrane in Figure 6(b) is equal to 200 nm, which is the same as the nominal value of the Cyclopore® substrate used. Therefore, the pore size on the membrane can be calculated with this methodology. The dimensions of the grafted ion-responsive polymer can be evaluated using the pore diameters of the grafted and nongrafted membranes. We can observe large dimensional changes of the ion-responsive grafted polymer in response to temperature and $BaCl_2$ concentration in every figure. In Figure 6(b) in particular, the dimensional change is more than 3-fold at relatively low filling ratios. Our methodology and this information will contribute to the applications and designs of the molecular recognition ion gating membranes.

Conclusions

A molecular recognition ion gating membrane having cylindrical straight pores was developed by grafting an ion-responsive polymer onto the pore surface of a polycarbonate track-etched membrane substrate. Successful preparation of the membrane was confirmed by its weight change, FT–IR, and SEM images. The permeation flux of pure water and an aqueous $BaCl_2$ solution through the membrane was measured, and the gating properties of the membrane were investigated and confirmed to be similar to those of membranes prepared with a PE porous substrate. The information about pore sizes of the ion gating membrane was obtained using the Hagen–Poiseuille equation. Our analysis of the grafted ion-responsive polymer size showed a polymer's large dimensional change in response to temperature and specific ion concentration.

Literature Cited

Friebe, A. and M. Ulbricht; "Controlled Pore Functionalization of Poly(Ethylene Terephthalate) Track-Etched Membranes via Surface-Initiated Atom Transfer Radical Polymerization," *Langmuir*, **23**, 10318–10322 (2007)

Ito, T., T. Hioki, T. Yamaguchi, T. Shinbo, S.-I. Nakao and S. Kimura; "Development of a Molecular Recognition Ion Gating Membrane

and Estimation of Its Pore Size Control," *J. Amer. Chem. Soc.*, **124**, 7840–7846 (2002)

Irie, M., Y. Misumi and T. Tanaka; "Stimuli-Responsive Polymers—Chemical-Induced Reversible Phase-Separation of an Aqueous-Solution of Poly(*N*-Isopropylacrylamide) with Pendent Crown-Ether Groups," *Polymer*, **34**, 4531–4535 (1993)

Rui, X., L.-Y. Chu, W.-M. Chen, W. Xiao, H.-D. Wang and J. B. Qu; "Characterization of Microstructure of Poly(*N*-Isopropylacrylamide)-Grafted Polycarbonate Track-Etched Membranes Prepared by Plasma-Graft Pore-Filling Polymerization," *J. Membr. Sci.*, **258**, 157–166 (2005)

Ungaro, R., E. B. Haj and J. Smid; "Substituent Effects on Stability of Cation Complexes of 4′-Substituted Monobenzo Crown Ethers," *J. Amer. Chem. Soc.*, **98**, 5198–5202 (1976)

Yagi, K., J. A. Ruitz, M. C. Sanchez and C. Guerrero; "Cation Binding-Properties of Polymethacrylamide Derivatives of Crown Ethers," *Macromol. Chem. Rapid Commun.*, **1**, 263–268 (1980)

Yamaguchi, T., S.-I. Nakao and S. Kimura; "Plasma-Graft Filling Polymerization—Preparation of a New Type of Pervaporation Membrane for Organic Liquid Mixtures," *Macromolecules*, **24**, 5522–5527 (1991)

Yamaguchi, T., S.-I. Nakao and S. Kimura; "Evidence and Mechanisms of Filling Polymerization by Plasma-Induced Graft Polymerization," *J. Polym. Sci. Part A: Polym. Chem.*, **34**, 1203–1208 (1996)

Yamaguchi, T., T. Ito, T. Sato, T. Shinbo and S. I. Nakao; "Response Mechanism of a Molecular Recognition Ion Gating Membrane," *J. Amer. Chem. Soc.*, **121**, 4078–4079 (1999)

Journal of Chemical Engineering of Japan, Vol. 42, No. 2, pp. 86–94, 2009 **Research Paper**

A New Free Volume Theory Based on Microscopic Concept of Molecular Collisions for Penetrant Self-Diffusivity in Polymers

Hidenori OHASHI, Taichi ITO and Takeo YAMAGUCHI
Chemical Resources Laboratory, Tokyo Institute of Technology, R1-17, 4259, Nagatsuta-cho, Midori-ku, Yokohama-shi, Kanagawa 226-8503, Japan

Keywords: Self-Diffusivity in Polymer, Free Volume Theory, Molecular Collisions, Quantum Chemical Calculation

A new free volume theory, which we named "shell-like free volume" theory, is developed for penetrant diffusivity in polymers by introducing microscopic concept of molecular collisions. Shell-like free volume is defined as the ambient free space of the penetrant molecule; it is consistent with the notion of molecular collisions, which is the microscopic origin of molecular diffusion. The microscopic notion can give physical meaning to all the parameters in the theory, and the parameters can be evaluated using the only pure-component parameters: the experimental viscosity of the solvent, the viscoelasticity of the polymer, and the molecular surface area estimated from the chemical structure using the semiempirical quantum chemical calculation. The predictive ability of the shell-like free volume theory is good for self-diffusivities of molecules with shapes from spherical to chain-like in polymer solutions over wide ranges of temperature and concentration.

Introduction

Molecular diffusivity is one of the most important dynamic physical properties to control device characteristics because it governs molecular transport in many processes and devices. In particular, penetrant molecular diffusivity through polymer materials is important in such applications as separation membranes (Yamaguchi *et al.*, 1991; Park and Paul, 1997; Merkel *et al.*, 2000; Ho and Poddar, 2001), cast-drying polymer coating processes (Wong *et al.*, 2005), and polymerization processes (Russell *et al.*, 1993; Tefera *et al.*, 1997). Practical use of the diffusivity can greatly facilitate device designs; however, one difficulty is that the dynamic property is a mixing property, which has a large number of combinations between constituents, polymers and diffusing molecules. Therefore, the molecular diffusivity in a polymer is desired to be estimated using only pure-component physical properties having a much smaller number. In order to accomplish the requirement and better expression of the transport property, a number of theoretical investigations including the friction (Cukier, 1984; Phillies, 1989), obstruction (Mackie and Meares, 1955; Ogston *et al.*, 1973), molecular (Pace and Datyner, 1979a, 1979b; Kloczkowski and Mark, 1989), and free volume models (Fujita, 1961; Vrentas and Duda, 1977a, 1977b) have been proposed (Muhr and Blashard, 1982; Tirrell, 1984; Masaro and Zhu, 1999) up until now.

In the present investigation, we develop a new model based on free volume theory (Doolittle, 1951; Doolittle and Doolittle, 1957). The well-defined physical image of free volume theory is that it is only when a free volume hole of sufficient size opens up next to a penetrant molecule that the molecule can jump into the hole and diffusion can occur. It was formulated by Cohen and Turnbull (1959) and other researchers (Liu *et al.*, 2002), and the notion has been widely extended to penetrant diffusion in polymer systems (Fujita, 1961; Vrentas and Duda, 1977a, 1977b; Paul, 1983). In these theories, the idea that both polymers and solvents contribute to the free volume of the system is highly successful, especially in the Vrentas–Duda model (Vrentas *et al.*, 1996; Vrentas and Vrentas, 1998) and the Cohen–Turnbull model (von Meerwall *et al.*, 1998, 1999, 2007). The Vrentas–Duda model has been extensively studied to express the temperature, concentration, and molecular shape dependency of self-diffusivity of various penetrants in polymers, by introducing the notion of a polymer jumping unit and the idea that asymmetric molecular shapes influence the free volume distribution (Vrentas and Duda, 1977a; Vrentas *et al.*, 1996). The Cohen–Turnbull model, extended by von Meerwall *et al.* (1998, 1999, 2007), can accurately express the self-diffusivity of *n*-alkanes and polyethylene in their binary systems over wide temperature and molecular weight ranges, by introducing such concepts as molecular chain end effects, polymer entanglement, and

Received on May 29, 2008; accepted on October 15, 2008.
Correspondence concerning this article should be addressed to T. Yamaguchi (E-mail address: yamag@res.titech.ac.jp).

constraint release. These theoretical successes prompted us to use the sophisticated idea of free volume contribution in the present study.

Reconsidering the molecular diffusion phenomenon from the microscopic viewpoint, it is evident that molecular random walk movement originates in molecular collisions with adjacent molecules. From this standpoint, diffusion in simple systems has been described by collision-based models (Lamm, 1954; Dullien, 1963; Vanbeije and Ernst, 1973; Dymond, 1974; Atkins, 1990). In fact, molecular collisions are also an important feature of molecular diffusion in polymer-containing systems. If the microscopic concept of molecular collision is introduced into the diffusion model for polymeric systems, it can contribute to a sophisticated model that can describe molecular diffusivity in polymers based on the microscopically fundamental notion, but no such model has been developed. In the present study, we suggest a novel microscopic notion named "shell-like free volume" by reexamining microscopic molecular collisions, and introduce the concept into the fundamental equation of free volume theory (Cohen and Turnbull, 1959; Liu *et al.*, 2002). Furthermore, the introduction of the microscopic concept finally enables estimation of the molecular diffusivity in a polymer as a mixing property, by using only pure-component physical properties. Then, by comparing experimental and calculated self-diffusivities of solvent molecules in polymers, the validity of the developed model is investigated.

1. Theory

1.1 A novel concept and definition of shell-like free volume

Molecular collisions create free space around a penetrant molecule, and only the contacting space is accessible for penetrant molecular motion, because a molecule drifts by colliding with adjacent molecules. In the present study, based on this microscopic idea, we developed a new concept, "shell-like free volume" around a molecule, as the amount of mean free space contacting the molecule (**Figure 1**). This shell-like free volume, referred to as D_s [cm^3/molecule], is taken as the free volume per molecule in the free volume basic equation, and the following formula for molecular diffusivity D_s [cm^2/s] is obtained.

$$D_s = D_0 \exp\left(-v^*/v_{f,slfv}\right) \tag{1}$$

where, D_s [cm^2/s] is a preexponential factor, and v^* [cm^3/molecule] is the critical molecular volume, which is the required space for a molecular diffusive jump. Usually, v^* is regarded as the volume occupied by a penetrant molecule at 0 K (Haward, 1970). The shell-like free volume $v_{f,SLFV}$ can be calculated as the product of penetrant molecular surface area s_1 [Å^2/molecule] (the unit is equal to 6.023×10^7 cm^2/mol in SI units and for the facilitation of actual calculation, the SI unit will be used hereafter) and free volume thickness δ [Å] (the unit is equal to 1×10^{-8} cm and the SI units will be used hereafter). The simple physical meaning of the parameter $v_{f,SLFV}$ is that as the space around the molecule increases, it becomes easier for the molecule to move. This image seems to agree reasonably well with actual images of molecular movement. Here, we note that our first target is the systems composed of nonpolar substances in which there is no strong interaction between the molecules that reduce molecular collisions.

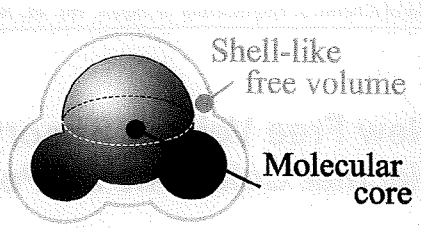

Fig. 1 Schematic illustration of "shell-like free volume" around a molecule

1.2 Calculation of shell-like free volume

Penetrant and polymer each have their own free volume $V_{f,i}/\gamma$ [cm^3/g] of component i (i = 1, 2, where the subscript 1 represents penetrant, such as solvent, and 2 represents polymer hereafter). The amount of free volume $V_{f,i}/\gamma$ is an inherent property of each substance, and it can be estimated directly using the substance's dynamic physical property, such as the rheological property of the pure component, as shown later in Section 2.4. The free volume thickness of each pure-component, δ_i [cm], can be calculated by dividing the inherent free volume amount [cm^3/g] by the molecular surface area [cm^2/g] (**Figure 2**).

$$\delta_i = \left(V_{f,i}/\gamma\right)/\left(s_i N_A/M_i\right) \tag{2}$$

where, s_i [cm^2/mol] and M_i [g/mol] represent the molecular surface area and molecular weight of component i, respectively, and N_A is Avogadro's number.

Using information about molecular surface area and free volume thickness, the shell-like free volume can be calculated. A penetrant molecule contacts with other molecules on its surface, and the contacting proportion is equal to a surface area fraction σ_i [cm^2/cm^2], expressed as shown in Eq. (3).

$$\sigma_i = \frac{\text{Summation of molecular surface area of component } i}{\text{Summation of surface area of all molecules included in system}} = \frac{\omega_i(s_i/M_i)}{\sum_j \omega_j(s_j/M_j)} \tag{3}$$

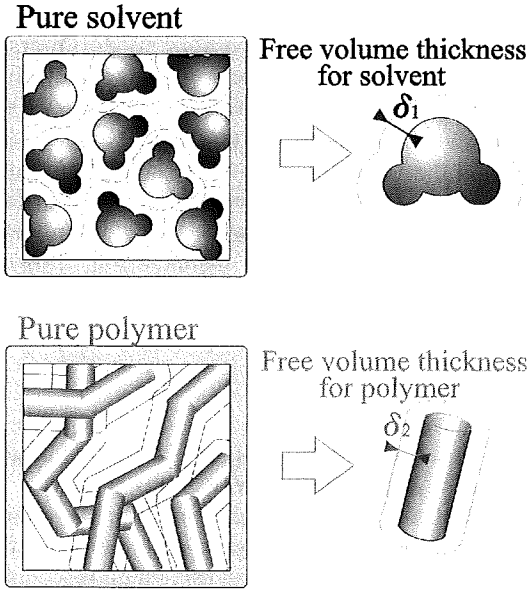

Fig. 2 Schematic illustration of free volume thickness of solvent and polymer; the free volume thickness of each component can be calculated by dividing the pure-component free volume $V_{f,i}/\gamma$ by its molecular surface area $s_i N_A/M_i$

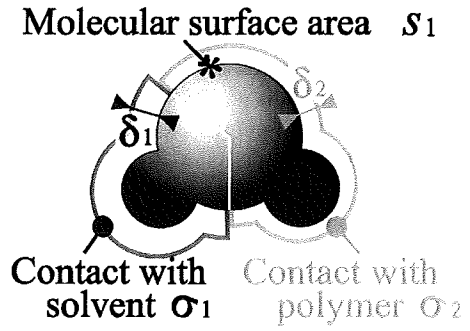

Fig. 3 The shell-like free volume can be calculated as the product of molecular surface area s_1 and free volume thickness; a penetrant molecule contacts the solvent over a surface area fraction σ_1 and contacts the polymer over the fraction σ_2; the free volume thickness assigned by the solvent is δ_1, and that assigned by the polymer is δ_2; the shell-like free volume $v_{f,SLFV}$ is therefore $s_1(\sigma_1\delta_1 + \sigma_2\delta_2)$

where, ω_i [g/g] represents the weight fraction of component i.

It is reasonable that the free volume thickness of each component δ_i should be assigned to the penetrant molecule in proportion to its corresponding surface area fraction σ_i (**Figure 3**) and the shell-like free volume can be calculated as shown in Eq. (4).

$$v_{f,SLFV} = s_1 \sum_i \sigma_i \delta_i \tag{4}$$

Thus, by combining Eqs. (1) to (4), the penetrant self-diffusivity in our model is shown by Eq. (5).

$$\begin{aligned} D_{s1} &= D_0 \exp\left(-v^*/v_{f,SLFV}\right) \\ &= D_0 \exp\left\{-\hat{V}_1^* M_1/N_A \Big/ s_1 \sum_i \left[\frac{\omega_i s_i/M_i}{\sum_j \omega_j (s_j/M_j)} \cdot \frac{(V_{f,i}/\gamma)}{s_i N_A M_i}\right]\right\} \\ &= D_0 \exp\left[-\frac{\hat{V}_1^* M_1 \sum_j \omega_j (s_j/M_j)}{s_1 \cdot \sum_i \omega_i (V_{f,i}/\gamma)}\right] \end{aligned} \tag{5}$$

where, $\hat{V}_1^*$ [cm³/g] is the critical volume of component i and can be calculated as $\hat{V}_1^* = v_1^* N_A/M_1$. In Eq. (5), $\sum\omega_i(V_{f,i}/\gamma)$ is the total free volume contained in the mixed system $V_{f,sys}/\gamma$ [cm³/g] (subscript i is used for the summation of free volume), and $N_A\sum\omega_j(s_j/M_j)$ is the total surface area of all molecules contained in the system S_{sys} [cm²/g] (subscript j is used for the summation of molecular surface area); thus, Eq. (5) can be rewritten as Eq. (6).

$$D_{s1} = D_0 \exp\left[-\frac{\hat{V}_1^* M_1/N_A}{s_1 \cdot (V_{f,sys}/\gamma S_{sys})}\right] \tag{6}$$

Equations (5) and (6) are the formulas for "shell-like free volume" theory.

To make a calculation using Eq. (5), values of the molecular surface area s_i and the free volume amount $V_{f,i}/\gamma$ of component i are required as model parameters. Estimation of the parameters is shown in the following sections.

1.3 Calculation of molecular surface area using a semiempirical quantum chemical calculation

A semiempirical quantum chemical calculation was used to estimate the molecular surface area of pure solvents and pure polymers from their chemical structures. A computer-aided chemistry modeling program, CAChe (Fujitsu Ltd.), was used for the whole calculation.

The computation procedure for the molecular surface area is as follows. First, one molecule was produced on the molecular structure console of CAChe. The constructed molecular structure was optimized by using the molecular mechanics calculation, and was then optimized using a semiempirical quantum chemical calculation; finally, the isoelectric surface and its surface area were calculated using a semiempirical calculation. The PM3 method was chosen as the semiempirical quantum chemical calculation method (Stewart, 1989; Dewar *et al.*, 1990), and an electron density of 0.0020 a.u. (1 a.u. is defined as 6.748 e/Å³)

was used as the definition of molecular surface contour. This isoelectric envelope contains 96% of all electrons (Bader *et al.*, 1987), and has been shown to be suitable for expressing the molecular surface, because the contour of 0.0020 a.u. describes the outer boundary of the molecule that contacts with other molecules (Pacios, 1995).

The molecular surface area for a solvent molecule s_1 can be directly estimated using the above procedure. However, for the polymer molecule, an additional calculation is necessary because of the existence of the polymer terminal groups. Here, an n-mer polymer is supposed to consist of two terminal units and $n - 2$ internal units, and the surface area of the n-mer is regarded as the sum of the surface areas of the two types of unit. The molecular surface area of the monomeric unit $s_{2,\text{mon}}$ [Å^2/monomeric unit] (the unit is equal to 6.023×10^7 cm^2/mol-monomeric unit and the SI units will be used hereafter) should correspond to that of an internal unit. The surface areas of 8-mer, 10-mer, and 12-mer polymers were calculated, and the internal unit surface area was obtained using an optimization algorithm.

The semiempirical quantum chemical calculation was carried out three times for each substance and the average values were used. Data deviation was less than 1% for solvent molecules and less than 4% for polymer molecules. In some cases of polymer molecule, there is electron cloud overlap among its side groups, which produces deviation of polymer surface area; therefore, folded conformations of polymers were avoided for the calculation.

1.4 Calculation of free volume

As noted above in Section 2.2, the free volume in the system is also an important parameter in the shell-like free volume theory, and to evaluate it, we followed the Vrentas–Duda free volume representation in which both polymers and solvents contribute to the free volume of the system (Vrentas and Duda, 1977a). Vrentas and Duda assumed that the free volume of component i, $V_{f,i}/\gamma$ [cm^3/g], has a linear temperature-dependent function as shown by Eq. (7).

$$V_{f,i}/\gamma = (K_{1i}/\gamma)(K_{2i} - T_{gi} + T) \tag{7}$$

where, (K_{1i}/γ) [cm^3/(g K)] and $(K_{2i} - T_{gi})$ [K] are the free volume parameters of component i. These parameters can be estimated using the rheological properties of the polymer and solvent. The solvent free volume parameters, (K_{11}/γ) and $(K_{21} - T_{g1})$, are calculated from the pure solvent viscosity data by combining the Dullien equation (Dullien, 1972; Chhabra, 1991) and the free volume theory. The polymer free volume parameters, (K_{12}/γ) and $(K_{22} - T_{g2})$, are connected to the Williams–Landel–Ferry (WLF) parameters (Ferry, 1970), which are estimated from polymer melt viscoelastic properties. These parameters were well estimated for various solvents and polymers by Zielinski, Hong, and other researchers (Zielinski and Duda, 1992; Hong, 1995; Yamaguchi *et al.*, 2003). Additivities of the free volumes can be assumed in a case of the combinations between nonpolar substances as our target, and thus, the free volume of a mixed system $V_{f,sys}/\gamma$ [cm^3/g] can be expressed as the summation of the free volumes of every component as shown by Eq. (8).

$$V_{f,sys}/\gamma = \sum_i \omega_i (V_{f,i}/\gamma) \tag{8}$$

1.5 Prediction of penetrant self-diffusivity in polymer using shell-like free volume theory

All of the parameters used in the calculation of shell-like free volume theory are pure-component parameters, and can be evaluated using their viscoelastic properties and semiempirical quantum chemical calculations. The predictive ability of the theory is validated by evaluating experimental self-diffusivity data. In this study, the following solvent–polymer binary systems were used for validation of shell-like free volume theory: benzene–polystyrene (Kosfeld and Zumkley, 1979), ethylbenzene–polystyrene (Kosfeld and Zumkley, 1979; Zgadzai and Maklakov, 1985), n-dodecane–polystyrene (Kim *et al.*, 1994), benzene–polyisobutylene (Kosfeld and Zumkley, 1979), toluene–polyisobutylene (Bandis *et al.*, 1995), and n-hexadecane–polyisobutylene (Moore and Ferry, 1962).

All the experimental self-diffusivity data values were measured at temperatures higher than the glass transition temperature of the relevant polymer, to assure the homogeneity of the system as the fundamental assumption of free volume theory. All parameters of each substance used in the calculation are tabulated in **Tables 1** and **2**.

2. Results and Discussion

2.1 Validation of shell-like free volume theory by comparing experimental and calculated penetrant self-diffusivities in polymer

Experimental and predicted solvent self-diffusivities are compared in **Figures 4–8**. As can be seen in all of the figures, the shell-like free volume theory gives excellent agreement for the self-diffusivity of solvent molecules in polymer solutions in middle to high solvent concentrations. However, in the n-dodecane–polystyrene and toluene–polyisobutylene systems in Figures 5 and 7, the deviations between experimental and calculated self-diffusivities are somewhat large in the low solvent concentration range. The deviation may mainly result from errors in free volumes. A small error in free volume tends to cause a large error in self-diffusivity because of the exponential

Table 1 Solvent parameters used in self-diffusivity prediction with shell-like free volume theory for penetrant in penetrant–polymer binary systems

	K_{11}/γ	$K_{21}-T_{g1}$	$\hat{V}_1^*$	M_1	D_0	s_1	
	[cm³/(g K)]	[K]	[cm³/g]	[g/mol]	[cm²/s]	[cm²/mol][a]	[Å²/molecule][b]
Benzene	1.51×10^{-3}	−94.32	0.901	78.1	4.47×10^{-4}	6.81×10^{9}	113.1
Toluene	2.20×10^{-3}	−102.72	0.917	94.1	1.87×10^{-4}	8.07×10^{9}	134.0
Ethylbenzene	2.22×10^{-3}	−100.08	0.928	106.2	1.54×10^{-4}	9.20×10^{9}	152.7
n-Dodecane	1.05×10^{-3}	−57.96	1.070	170.3	6.13×10^{-4}	1.70×10^{10}	281.5
n-Hexadecane	0.83×10^{-3}	−53.66	1.053	226.5	7.33×10^{-4}	2.18×10^{10}	361.8

[a]Shown in SI units; [b]Shown in microscopic units;
Unit conversion: 1 [Å²/molecule] = 6.023×10^{7} [cm²/mol]

Table 2 Polymer parameters used in self-diffusivity prediction with shell-like free volume theory for penetrant in penetrant–polymer binary systems

	K_{12}/γ	$K_{22}-T_{g2}$	$\hat{V}_2^*$	$M_{2,\mathrm{mon}}$	T_{g2}	$s_{2,\mathrm{mon}}$	
	[cm³/(g K)]	[K]	[cm³/g]	[g/mol]	[K]	[cm²/mol-monomeric unit][a]	[Å²/monomeric unit][b]
Polystyrene	5.82×10^{-4}	−327.0	0.850	104	373	5.95×10^{9}	98.8
Polyisobutylene	2.51×10^{-4}	−100.6	1.004	56	205	3.30×10^{9}	54.7

[a]Shown in SI units; [b]Shown in microscopic units;
Unit conversion: 1 [Å²/monomeric unit] = 6.023×10^{7} [cm²/mol-monomeric unit]

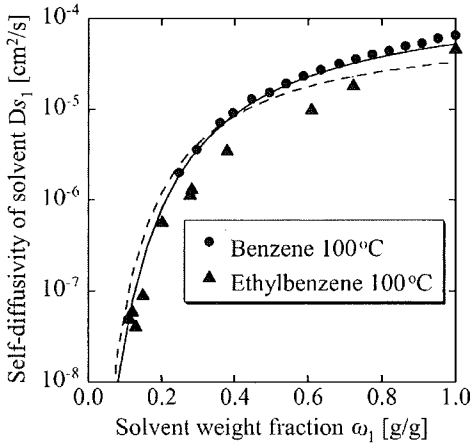

Fig. 4 Penetrant self-diffusivities in polystyrene solution; ● is the experimental self-diffusivity of benzene in the benzene–polystyrene binary system, and ▲ is that of ethylbenzene in the ethylbenzene–polystyrene binary system; the solid line shows the prediction for benzene, and the broken line is for ethylbenzene; lines are predicted using shell-like free volume theory

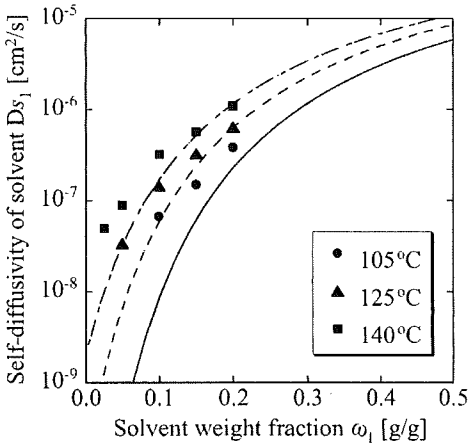

Fig. 5 *n*-Dodecane self-diffusivity in polystyrene solution; ●, ▲, and ■ are experimental self-diffusivities of *n*-dodecane in the *n*-dodecane–polystyrene binary system at temperatures of 105, 125, and 140°C, respectively; the solid line represents the prediction for 105°C, the broken line for 125°C, and the dashed–dotted line for 140°C

term in the fundamental free volume equation Eq. (1), especially in the region of small free volumes; thus, more precise parameters are required to attain more precise calculation. With these exceptions, the shell-like free volume theory can successfully estimate the self-diffusivities of every penetrant molecule in both polymers over wide temperature and composition ranges. This certainly reflects the validity of the microscopic notion that it is the contacting free space that is available for penetrant molecular diffusive motion.

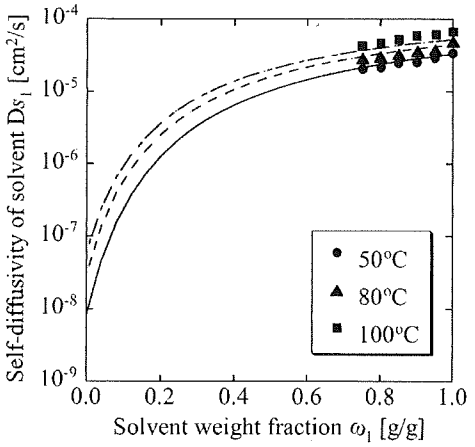

Fig. 6 Benzene self-diffusivity in polyisobutylene solution; ●, ▲, and ■ are experimental self-diffusivities of benzene in the benzene–polyisobutylene binary system at temperatures of 50, 80, and 100°C, respectively; the solid line represents the prediction for 50°C, the broken line for 80°C, and the dashed–dotted line for 100°C

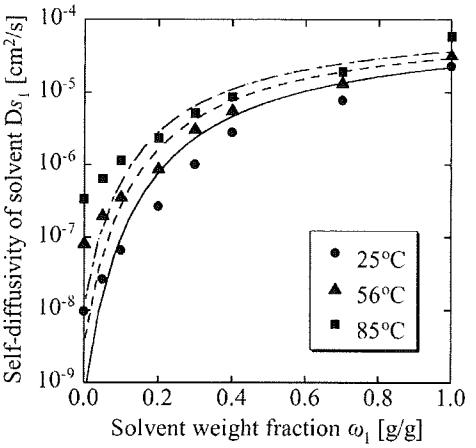

Fig. 7 Toluene self-diffusivity in polyisobutylene solution; ●, ▲, and ■ are experimental self-diffusivities of toluene in the toluene–polyisobutylene binary system at temperatures of 25, 65, and 85°C, respectively; the solid line represents the prediction for 25°C, the broken line for 56°C, and the dashed–dotted line for 85°C

The developed model can predict without the use of an arbitrary adjustable parameter due to the successful introduction of the microscopic notion of the molecular collisions. Nevertheless, the practical estimation accuracy of our model was found to be equal or even better than those of other models over a wide range of temperatures, compositions, and molecular shapes. The detailed and careful comparative calculations between the model and other models will be summarized in another paper.

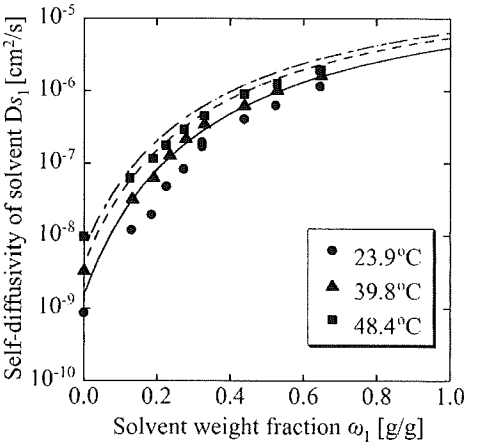

Fig. 8 *n*-Hexadecane (cetane) self-diffusivity in polyisobutylene solution; ●, ▲, and ■ are experimental self-diffusivities of cetane in the cetane–polyisobutylene binary system at temperatures of 23.9, 39.8, and 48.4°C, respectively; the solid line represents the prediction for 23.9°C, the broken line for 39.8°C, and the dashed–dotted line for 48.4°C

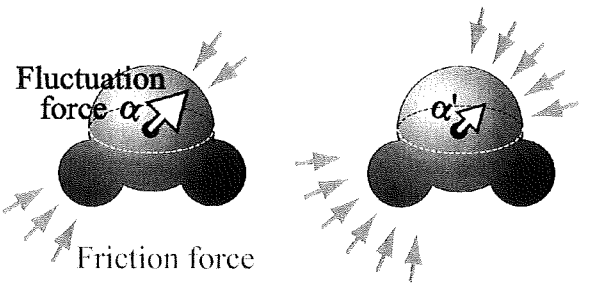

Fig. 9 Schematic of fluctuation force imposed on a penetrant molecule; when the friction frequency is small, the fluctuation force α is large (left); on the other hand, when the friction frequency is large, the fluctuation force α' becomes small because the friction force imposed on the penetrant molecule from various directions is averaged out (right)

2.2 Consideration of shell-like free volume in terms of molecular collisions

As described above, molecular diffusion originates in collisions between molecules (Cussler, 1977). Detailed consideration of shell-like free volume in terms of molecular collisions is given. This relationship can be discussed in terms of molecular surface area and free volume thickness, the constituents of the shell-like free volume.

When the molecular surface area is large, the collision frequency of the penetrant molecule is large. In this case, the fluctuation force α [N s/m molecule] for the molecule becomes small, because the frictional

force is imposed on the penetrant from various directions, and thus the fluctuation force is averaged out (**Figure 9**). Molecular self-diffusivity and the fluctuation force imposed on the molecule can be related by Einstein's relation (Kubo *et al.*, 1985) shown as Eq. (9).

$$D_s = \frac{kT}{\alpha} \tag{9}$$

This is derived from nonequilibrium statistical mechanics, where k [J/(molecule K)] denotes the Boltzmann coefficient. From this equation, larger molecular surface areas imply faster molecular diffusion, that is, from the standpoint of the molecular surface area, the relationship between shell-like free volume and self-diffusivity is validated by considering molecular collisions.

On the other hand, when the free volume thickness is large, the mean distance between collisions becomes longer. Self-diffusivity can also be roughly described as shown by Eq. (10).

$$D_s = \frac{d^2}{6\tau} = \frac{d \cdot u}{6} \tag{10}$$

This is the formula for self-diffusivity of a random walk jumping motion, where d [cm] is the mean molecular jumping distance between molecular collisions, τ [s] is the mean time required to carry out one jump, and u [cm/s] represents the mean molecular kinetic velocity. The mean molecular velocity is constant at constant temperature because it is determined by the mean kinetic energy of the molecule. Thus, it is easy to see that larger distances between molecules imply larger molecular self-diffusivities. Therefore, in relation to the free volume thickness, the relationship between shell-like free volume and self-diffusivity is validated using the concept of molecular collisions.

2.3 Advantages of the shell-like free volume theory

The shell-like free volume equation Eq. (5) includes only pure-component parameters, and these parameters can be evaluated using the components' viscoelastic properties and semiempirical quantum chemical calculations. This means that the shell-like free volume equation can predict penetrant self-diffusivity with only known pure-component parameters, without using any arbitrary adjustable parameters. Reconsideration of diffusive motion in terms of microscopic molecular collisions gives physical meanings to all of the parameters included in the theory.

The discussion is applicable to penetrant molecules with shapes ranging from spherical to long chains, and this is the correct microscopic explanation of why the present model can predict self-diffusivities of various types of penetrant molecules in a polymer matrix so well. Molecular collisions are a common mechanism for diffusion of various types of penetrants in polymers; thus, the shell-like free volume theory has the potential to predict gas molecular diffusion in polymers and diffusion in ternary systems, which we are currently pursuing.

Conclusions

We have developed a novel microscopic concept of "shell-like free volume" around a molecule. The simple but comprehensive notion is that the contacting free space is the space available for the diffusive jumping motion of a penetrant molecule. The concept is associated with the microscopic notion of molecular collisions from the viewpoints of both molecular surface area and free volume thickness, the constituents of the shell-like free volume. All of the parameters used in shell-like free volume theory have physical meaning based on microscopic concepts, and can be evaluated using only pure-component properties: the free volume can be obtained from experimental rheological data, i.e. viscosity for the solvent and viscoelasticity for the polymer, and molecular surface area is obtained using the semiempirical quantum chemical calculation. Thus, the developed model can predict penetrant self-diffusivity in a polymer without using any arbitrary adjustable parameters. The developed model accurately predicts the self-diffusivity of molecules with shapes ranging from spherical to long chains in polymer solutions over wide ranges of temperature and concentration. These results show the validity of the microscopic concept of the shell-like free volume.

Nomenclature

D_0	=	preexponential factor	[cm²/s]
D_s	=	self-diffusivity of penetrant molecule	[cm²/s]
d	=	mean molecular jumping distance between molecular collisions	[cm]
K_{1i}/γ	=	free volume parameters of component i	[cm³/g K]
$K_{2i} - T_{gi}$	=	free volume parameters of component i	[K]
k	=	the Boltzmann coefficient	[J/(molecule K)]
N_A	=	the Avogadro's number	[molecules/mol]
S_{sys}	=	total surface area of all molecules contained in the system	[cm²/g]
s_i	=	molecular surface area of component i	[Å²/molecule]
T	=	temperature of the system	[K]
u	=	mean molecular kinetic velocity	[cm/s]
$\hat{V}^*$	=	critical volume of penetrant, $=v_1^* N_A/M_1$	[cm³/g]
$V_{f,i}/\gamma$	=	free volume of component i	[cm³/g]
$V_{f,sys}/\gamma$	=	total free volume contained in the system	[cm³/g]
v^*	=	critical molecular volume of penetrant molecule	[cm³/molecule]
$v_{f,SLFV}$	=	shell-like free volume of penetrant molecule	[cm³/molecule]
α	=	fluctuation force	[N s/m molecule]
δ_i	=	free volume thickness of component i	[cm]
τ	=	mean time required to carry out one diffusive jump	[s]
σ_i	=	surface area fraction of component i	[cm²/cm²]
ω_i	=	weight fraction of component i	[g/g]

Literature Cited

Atkins, P. W.; Physical Chemistry, 4th ed., Oxford University Press, Oxford, U.K. (1990)

Bader, R. F. W., M. T. Carroll, J. R. Cheeseman and C. Chang; "Properties of Atoms in Molecules—Atomic Volumes," *J. Am. Chem. Soc.*, **109**, 7968–7979 (1987)

Bandis, A., P. T. Inglefield, A. A. Jones and W.-Y. Wen; "A Nuclear-Magnetic-Resonance Study of Dynamics in Toluene-Polyisobutylene Solutions. 1. Penetrant Diffusion and Fujita Theory," *J. Polym. Sci. Part B: Polym. Phys.*, **33**, 1495–1503 (1995)

Chhabra, R. P.; "Effect of Pressure on Self-Diffusion in Liquids," *Int. J. Thermophys.*, **12**, 153–161 (1991)

Cohen, M. H. and D. Turnbull; "Molecular Transport in Liquids and Glassses," *J. Chem. Phys.*, **31**, 1164–1169 (1959)

Cukier, R. I.; "Diffusion of Brownian Spheres in Semidilute Polymer-Solutions," *Macromolecules*, **17**, 252–255 (1984)

Cussler, E. L.; Diffusion, Mass Transfer in Fluid Systems, 2nd ed., Cambridge University Press, New York, U.S.A. (1977)

Dewar, M. J. S., E. F. Healy, A. J. Holder and Y.-C. Yuan; "Comments on a Comparison of AM1 with the Recently Developed PM3 Method," *J. Comput. Chem.*, **11**, 541–542 (1990)

Doolittle, A. K.; "Studies in Newtonian Flow. II. The Dependence of the Viscosity of Liquids on Free-Space," *J. Appl. Phys.*, **22**, 1471–1475 (1951)

Doolittle, A. K. and D. B. Doolittle; "Studies in Newtonian Flow. V. Further Verification of the Free-Space Viscosity Equation," *J. Appl. Phys.*, **28**, 901–905 (1957)

Dullien, F. A. L.; "New Relationship between Viscosity and Diffusion Coefficients Based on Lamms Theory of Diffusion," *Trans. Faraday Soc.*, **59**, 856–868 (1963)

Dullien, F. A. L.; "Predictive Equations for Self-Diffusion in Liquids—Different Approach," *AIChE J.*, **18**, 62–70 (1972)

Dymond, J. H.; "Corrected Enskog Theory and Transport-Coefficients of Liquids," *J. Chem. Phys.*, **60**, 969–973 (1974)

Ferry, J. D.; Viscoelastic Properties of Polymers, 2nd ed., Wiley, New York, U.S.A. (1970)

Fujita, H.; "Diffusion in Polymer-Dilluent Systems," *Fortschr. Hochpolym.—Forsch.*, **3**, 1–47 (1961)

Haward, R. N.; "Occupied Volume of Liquids and Polymers," *J. Macromol. Sci. Rev. Macromol. Chem. Phys.*, **C4**, 191–242 (1970)

Ho, W. S. W. and T. K. Poddar; "New Membrane Technology for Removal and Recovery of Chromium from Waste Waters," *Environ. Prog.*, **20**, 44–52 (2001)

Hong, S.-U.; "Prediction of Polymer-Solvent Diffusion Behavior Using Free-Volume Theory," *Ind. Eng. Chem. Res.*, **34**, 2536–2544 (1995)

Kim, D., J. M. Caruthers, N. A. Peppas and E. von Meerwall; "Self-Diffusion and Mutual-Diffusion Coefficients in the Dodecane Polystyrene System," *J. Appl. Polym. Sci.*, **51**, 661–668 (1994)

Kloczkowski, A. and J. E. Mark; "On the Pace—Datyner Theory of Diffusion of Small Molecules through Polymers," *J. Polym. Sci. Part B: Polym. Phys.*, **8**, 1663–1674 (1989)

Kosfeld, R. and L. Zumkley; "Mobility of Small Molecules in Polymer Systems," *Ber. Bunsen Ges. Phys. Chem.*, **83**, 392–396 (1979)

Kubo, R., M. Toda and N. Hashitsume; Nonequilibrium Statistical Mechanics, 2nd ed., Springer-Verlag, Berlin, Germany (1985)

Lamm, O.; "The Formal Theory of Diffusion, and Its Relation to Self-Diffusion, Sedimentation Equilibrium, and Viscosity," *Acta Chem. Scand.*, **8**, 1120–1128 (1954)

Liu, H. Q., C. M. Silva and E. A. Macedo; "Generalised Free-Volume Theory for Transport Properties and New Trends about the Relationship between Free Volume and Equations of State," *Fluid Phase Equilib.*, **202**, 89–107 (2002)

Mackie, J. S. and P. Meares; "The Diffusion of Electrolytes in a Cation-Exchange Resin Membrane. I. Theoretical," *Proc. R. Soc. London, Ser. A*, **232**, 498–509 (1955)

Masaro, L. and X. X. Zhu; "Physical Models of Diffusion for Polymer Solutions, Gels and Solids," *Prog. Polym. Sci.*, **24**, 731–775 (1999)

Merkel, T. C., V. I. Bondar, K. Nagai, B. D. Freeman and I. Pinnau; "Sorption and Transport of Hydrocarbon and Perfluorocarbon Gases in Poly(1-trimethylsilyl-1-propyne)," *J. Polym. Sci. Part B: Polym. Phys.*, **38**, 415–434 (2000)

Moore, R. S. and J. D. Ferry; "Diffusion of Radioactively Tagged Cetane in Polyisobutylene–Cetane Mixtures and in Three Methacrylate Polymers," *J. Phys. Chem.*, **66**, 2699–2704 (1962)

Muhr, A. H. and J. M. V. Blanshard; "Diffusion in Gels," *Polymer*, **23**, 1012–1026 (1982)

Ogston, A. G., B. N. Preston and J. D. Wells; "Transport of Compact Particles through Solutions of Chain-Polymers," *Proc. R. Soc. London A*, **333**, 297–316 (1973)

Pace, R. J. and A. Datyner; "Statistical Mechanical Model for Diffusion of Simple Penetrants in Polymers. 1. Theory," *J. Polym. Sci. Part B: Polym. Phys.*, **17**, 437–451 (1979a)

Pace, R. J. and A. Datyner; "Statistical Mechanical Model of Diffusion of Complex Penetrants in Polymers. 1. Theory," *J. Polym. Sci. Part B: Polym. Phys.*, **17**, 1675–1692 (1979b)

Pacios, L. F.; "Atomic Radii Scales and Electron Properties Deduced from the Charge-Density," *J. Comput. Chem.*, **16**, 133–145 (1995)

Park, J. Y. and D. R. Paul; "Correlation and Prediction of Gas Permeability in Glassy Polymer Membrane Materials via a Modified Free Volume Based Group Contribution Method," *J. Membr. Sci.*, **125**, 23–39 (1997)

Paul, C. W.; "A Model for Predicting Solvent Self-Diffusion Coefficients in Nonglassy Polymer Solvent Solutions," *J. Polym. Sci. Part B: Polym. Phys.*, **21**, 425–439 (1983)

Phillies, G. D. J.; "The Hydrodynamic Scaling Model for Polymer Self-Diffusion," *J. Phys. Chem.*, **93**, 5029–5039 (1989)

Russell, G. T., R. G. Gilbert and D. H. Napper; "Chain-Length-Dependent Termination Rate Processes in Free-Radical Polymerizations. 2. Modeling Methodology and Application to Methyl-Methacrylate Emulsion Polymerizations," *Macromolecules*, **26**, 3538–3552 (1993)

Stewart, J. J. P.; "Optimization of Parameters for Semiempirical Method. 1. Method," *J. Comput. Chem.*, **10**, 209–220 (1989)

Tefera, N., G. Weickert and K. R. Westerterp; "Modeling of Free Radical Polymerization up to High Conversion. 2. Development of a Mathematical Model," *J. Appl. Polym. Sci.*, **63**, 1663–1680 (1997)

Tirrell, M.; "Polymer Self-Diffusion in Entangled Systems," *Rubber Chem. Technol.*, **57**, 523–556 (1984)

Vanbeije, H. and M. H. Ernst; "Modified Enskog Equation," *Physica*, **68**, 437–456 (1973)

von Meerwall, E., S. Beckman, J. Jang and W. L. Mattice; "Diffusion of Liquid *n*-Alkanes: Free-Volume and Density Effects," *J. Chem. Phys.*, **108**, 4299–4304 (1998)

von Meerwall, E., E. J. Feick, R. Ozisik and W. L. Mattice; "Diffusion in Binary Liquid *n*-Alkane and Alkane-Polyethylene Blends," *J. Chem. Phys.*, **111**, 750–757 (1999)

von Meerwall, E. D., N. Dirama and W. L. Mattice; "Diffusion in Polyethylene Blends: Constraint Release and Entanglement Dilution," *Macromolecules*, **40**, 3970–3976 (2007)

Vrentas, J. S. and J. L. Duda; "Diffusion in Polymer-Solvent Systems. 1. Re-Examination of Free-Volume Theory," *J. Polym. Sci. Part B: Polym. Phys.*, **15**, 403–416 (1977a)

Vrentas, J. S. and J. L. Duda; "Diffusion in Polymer-Solvent Systems. 2. Predictive Theory for Dependence of Diffusion-Coefficients on Temperature, Concentration, and Molecular-Weight," *J. Polym. Sci. Part B: Polym. Phys.*, **15**, 417–439 (1977b)

Vrentas, J. S. and C. M. Vrentas; "Predictive Methods for Self-Diffusion and Mutual Diffusion Coefficients in Polymer-Solvent Systems," *Eur. Polym. J.*, **34**, 797–803 (1998)

Vrentas, J. S., C. M. Vrentas and N. Faridi; "Effect of Solvent Size on Solvent Self-Diffusion in Polymer-Solvent Systems," *Macromolecules*, **29**, 3272–3276 (1996)

Wong, S.-S., T. A. Altinkaya and S. K. Mallapragada; "Understanding the Effect of Skin Formation on the Removal of Solvents from Semicrystalline Polymers," *J. Polym. Sci. Part B: Polym. Phys.*, **43**, 3191–3204 (2005)

Yamaguchi, T., S. Nakao and S. Kimura; "Plasma-Graft Filling Polymerization Preparation—Preparation of a New Type of Pervaporation Membrane for Organic Liquid-Mixtures," *Macromolecules*, **24**, 5522–5527 (1991)

Yamaguchi, T., B.-G. Wang, E. Matsuda, S. Suzuki and S.-I. Nakao; "Prediction and Estimation of Solvent Diffusivities in Polyacrylate and Polymethacrylates," *J. Polym. Sci. Part B: Polym. Phys.*, **41**, 1393–1400 (2003)

Zgadzai, O. E. and A. I. Maklakov; "Solvent Self-Diffusion in the System Polystyrene–Ethylbenzene in Terms of the Modified Free-Volume Theory," *Acta Polym.*, **11**, 621–623 (1985)

Zielinski, J. M. and J. L. Duda; "Predicting Polymer Solvent Diffusion-Coefficients Using Free-Volume Theory," *AIChE J.*, **38**, 405–415 (1992)